Supplemental Material

Disabled homolog 2 controls macrophage phenotypic polarization and adipose tissue inflammation

Samantha E. Adamson, Rachael Griffiths, Radim Moravec, Subramanian Senthivinayagam, Garren Montgomery, Wenshu Chen, Jenny Han, Poonam R. Sharma, Garrett R. Mullins, Stacey A. Gorski, Jonathan A. Cooper, Alexandra Kadl, Kyle Enfield, Thomas J. Braciale, Thurl E. Harris, Norbert Leitinger

R.G. and S.E.A. contributed equally to the study.

Supplemental Figure Legends

Supplemental Figure 1: Dab2 expression is differentially regulated in M1 and M2 macrophages. (**A**) Microarray analysis was performed after treating BMDM with either M1 stimuli LPS and IFNγ, or the M2 stimulus IL-4 for 3 hours(1). Screening for genes that are differentially regulated in M1 and M2 macrophages revealed *Dab2* among a group of genes that are upregulated in M2, but downregulated in M1 macrophages (also including the zinc finger protein Zfp36L1, cannabinoid receptor 2, inhibitor of differentiation Id1, and Zfp703, some of which have previously been implicated in the control of macrophage activation(2) (3)). (**B**) *Il6* (M1 marker) and *Arg1* (M2 marker) expression were quantified and normalized to *β2m* mRNA. Results are presented as relative to those of M0. Data are representative of 3 independent experiments. *P < 0.05 students t-test (mean ± s.e.m. of quadruplicate treatments). (**C**) *Dab2* expression was measured in BMDM isolated from a C56Bl/6 mouse and treated with 10 µg/ml LTA or 1 µg/ml LPS for up to 8hr. Results are normalized to *β2m* mRNA and are presented as relative to untreated cells. *P<0.0006 by 2-way ANOVA with Sidak's multiple comparison test. (**D**) Irf8 mRNA (left) and protein (right) expression was quantified in RAW 264.7 M0, M1, and M2 polarized macrophages. Western blot (right) demonstrates dab2 protein levels in M0, M1, and M2 polarized RAW 264.7 macrophages (8 h). Actin serves as a loading control. (**E**) Dab2 protein stability was measured by immunoblot of lysates of RAW 264.7 macrophages that were untreated or treated with 100 ng/ml LPS in the presence of 10 µg/ml cycloheximide, a protein synthesis inhibitor over a 12 h time course. GAPDH serves as a loading control. Quantification of three independent experiments is shown on the right. *P<0.05 by student's t-test.

Supplemental Figure 2: Manipulation of Dab2 expression by siRNA and expression plasmids. (**A**) RAW 264.7 macrophages were transfected with control or *Dab2* siRNA for 48 h. *Upper pane l*- Immunoblot analysis of Dab2 protein expression with GAPDH serving as a loading control. *Lower panel* - qRT-PCR analysis of *Dab2* mRNA expression, normalized to *β2m* mRNA. Data is presented as mean ± s.e.m. of quadruplicate treatments. (**B**) RAW264.7 macrophages were transfected with pCGT or pCGT-Dab2 for 48 h. *Upper panel* - Immunoblot analysis of Dab2 protein expression with GAPDH serving as a loading control. *Lower panel* - qPCR analysis of *Dab2* mRNA expression was normalized to *β2m* mRNA. Data is presented as mean ± s.e.m. of quadruplicate treatments. (**C**) qPCR analysis of *Dab2* levels normalized to *β2m* in resting cells transfected with pCGT, *p67 Dab2,* or *p96 Dab2*. (**D**) qPCR analysis of *Dab2* levels normalized to *β2m* in RAW 264.7 macrophages transfected with pCGT, *p67 Dab2,* or *p96 Dab2* and treated with IFNγ for 16 h or TNFα for 4 h. *P<0.05 significantly different from pCGT. $^{\#}$P<0.05 significantly different from control.

Supplemental Figure 3: Analysis of cellular composition of blood in *Dab2$^{fl/fl}$* and *Dab2$^{fl/fl}$LysM^{Cre}* mice. Whole blood composition was examined by Hemavet analyzer. (**A**) Cell number in K/μl and percent distribution of white blood cells (WBC), neutrophils (NE), lymphocytes (LY), monocytes (MO), eosinophils (EO), and basophils (BA). Data are shown as mean ± s.e.m.; n = 7 *for Dab2$^{fl/fl}$*, n = 6 for *Dab2$^{fl/fl}$LysM^{Cre}*. (**B and C**) White blood cells stained with CD45-APC-Cy7, CD11b-PerCP-Cy5.5, Ly6G-APC, Siglec F-PE, and Ly6C-FITC were subjected to FACS analysis. (**B**) Percentage of $CD45^+CD11b^+Ly6G^+$ (neutrophils NE; n=4), and $CD45^+CD11b^+SiglecF^+$ (eosinophils EO; *n* = 4) cells. Data is presented as mean ± s.e.m. (**C**) Representative gating of $CD45^+CD11b^+Ly6c\text{-}SSC^{lo}$ monocytes analyzed for $Ly6c^{hi}$, $Ly6c^{int}$, $Ly6c^{lo}$ expression (left two panels). Data points shown in the quantification (right three panels) represent individual animals (mean ± s.d. *n* = 4). (**D**) Peritoneal lavage cell number as determined by hemocytometer from LPS treated *Dab2$^{fl/fl}$* and *Dab2$^{fl/fl}$LysM^{Cre}* mice. Each point represents one mouse. Data is expressed as mean +/- s.e.m.

Supplemental Figure 4: Quantitative RT-PCR analysis of *Il1β*, *Il6,* and *Tnfα* mRNA expression in *Dab2$^{fl/fl}$* and *Dab2$^{fl/fl}$LysM^{Cre}* BMDM treated for 6 h with 200 μM palmitate (**A**) or 100 ng/ml TNFα (**B**). Results are normalized to *β2m.* *P<0.05 by student's t-test.

Supplemental Figure 5: (**A**) *Dab2$^{fl/fl}$* and *Dab2$^{fl/fl}$LysM^{Cre}* mice (n = 8 and n = 6, respectively) were fed a high fat diet [60% kcal from fat, 0.2% cholesterol (Bioserv)] for 12 weeks and blood was analyzed for WBC content by Hemavet, revealing no difference in absolute cell numbers or distribution. (**B** and **C**) Weight gain is shown for high fat diet fed, female *Dab2$^{fl/fl}$* (n=14) and *Dab2$^{fl/fl}$LysM^{Cre}* (n=9) mice (**B**) and age-matched, chow fed, female *Dab2$^{fl/fl}$* (n=5) and *Dab2$^{fl/fl}$LysM^{Cre}* (n=6) mice (**C**). (**D**) Flow cytometry gating strategy for isolated cells from adipose stromal vascular fraction: Cells were stained with CD45-APC-Cy7, CD11b-FITC, CD206-PE and CD11c-AF647 antibodies. Gating strategy 1 (for Fig 5D and E) shows cells gated by $CD45^+/CD11b^+$ (corresponding FMOs shown below). Next, $CD45^+/CD11b^+$ cells were assessed by $CD11c^+$ versus $CD206^+$ and gated as $CD11c^+$ or $CD206^+$ based on corresponding FMOs shown below. MFI for either CD11c or CD206 was determined for $CD45^+/CD11b^+$ cells. Gating Strategy 2 (for Fig 5F and G): First, $CD45^+$ cells were gated (CD45 FMO shown below) and next gated by $CD11b^+$ (CD11b FMO shown below). (**E**) Absolute number of $CD45^+/CD11b^+/CD11c^+$ cells per gram adipose tissue processed. (**F**) Absolute number of $CD45^+/CD11b^+/CD206^+$ cells per gram adipose tissue processed. For (**E**,**F**) data is presented as mean ± s.e.m. *P < 0.05 by Student's t-test. (**G**) *Dab2$^{fl/fl}$* and *Dab2$^{fl/fl}$LysM^{Cre}* mice were fed either a regular chow (Teklad) (n = 5 and n = 6, respectively) or a high fat diet [60% kcal from fat, 0.2% cholesterol (Bioserv)] (n = 9 and n = 14, respectively) for 12 weeks. Fasting glucose levels were measured every other week over the time of feeding by glucometer sampling of tail blood after 6 hour fast. (**H**) Glucose tolerance tests and (**I**) insulin tolerance tests in *Dab2$^{fl/fl}$* and *Dab2$^{fl/fl}$LysM^{Cre}* mice that were fed a regular chow diet. Mice were fasted 6 hours and injected intraperitoneally (i.p.) with a 1 g/kg glucose bolus for glucose tolerance test or 0.75 U/kg insulin for insulin tolerance test at time 0, and blood glucose levels were measured from tail blood by glucometer. Data was analyzed by area under the curve (AUC) analysis revealing no difference in glucose tolerance between chow fed *Dab2$^{fl/fl}$* mice and *Dab2$^{fl/fl}$LysM^{Cre}* mice. Data is presented as mean ± s.e.m. (n = 5 or 6 for GTT, n = 3 for ITT).

Supplemental Figure 6: Confocal microscopy of control and LPS treated bone marrow-derived macrophages isolated from *Dab2$^{fl/fl}$* mice shows nuclei in blue (Dapi), p65 in green, and Dab2 in red. Bottom panels represent analysis of z-stack images such that the y-axis is intensity of staining. Blue lines represent Dapi staining and show a peak in the middle, representing the nucleus. In untreated macrophages, p65 staining (green line) is evenly distributed along the cell, while in LPS treated macrophages, p65 staining (green line) aligns with Dapi

staining (blue line), indicating the presence of p65 in the nucleus in LPS-treated macrophages. Dab2 staining (red line) is evenly distributed along the cell in both untreated and LPS-treated macrophages, indicating that Dab2 does not enter the nucleus upon LPS treatment.

Supplemental Table 1: TRAF6 binding site consensus sequence in shown as well as two putative TRAF6 binding sites in murine Dab2 at amino acid position 226 and 689 which are conserved in human Dab2. NUMBL is a related TRAF6-binding adaptor protein that contains two conserved TRAF6 binding sites(4, 5).

ONLINE METHODS

Coimmunoprecipitation and immunoblot analysis- For immunoblots, cells were harvested in RIPA buffer supplemented with protease inhibitor cocktail (Roche) and phosphatase inhibitors (Sigma). Lysates were cleared by centrifugation at 12,000 g for 10 min at 4^{o}C then subjected to protein assay (Pierce). Proteins were separated on 10% SDS-PAGE and transferred to nitrocellulose membrane (BioRad). Membranes were incubated with Odyssey Licor blocking buffer or 5% BSA-TBS-Tween (phospho antibodies) for 1 h at room temperature. For immunoprecipitation, cells were either lysed in Lysis Buffer 1: 200 mM NaCl, 50 mM Tris HCL pH 8.8, 1% triton-x100, 0.5% sodium DOC, 0.1% SDS with phosphatase and protease inhibitor cocktails or Lysis Buffer 2: 137 mM NaCl,20 mM Tris HCL pH 7.5, 2 mM EDTA, 10% Glycerol, 1% Triton-X100 along with phosphatase and protease inhibitor cocktails. Lysate was passed through a 21G needle and incubated on ice for 10 min before clearing by centrifugation for 10 min in the presence of CL4B sepharose. Cleared cell lysates were incubated with premixed antibody/beads overnight at 4^{o}C followed by 3 washes in lysis buffer. Premixed antibody/beads: anti-TRAF6 or antibody (10 µl/sample) was mixed with 20 µl of Protein G Agarose beads (Pierce-20398) for 3-4 h. Final immunoprecipitates were resuspended in 20 µl of SDS-PAGE Laemmli buffer and resolved by SDS-PAGE followed by transfer to nitrocellulose membranes. Antibodies used were: Dab2, IκBα, phospho-IκBα, ICSBP (IRF8), p65, GAPDH, β-tubulin (Santa Cruz Biotechnology), Ser536-p65 (Cell Signaling), Actin (Sigma Aldrich). Anti-Rabbit T180/Y182 p38 (Cell Signaling Technologies-#4552S), anti-Rabbit p38 (Cell Signaling Technologies-#9212S), anti-Rabbit S536 p65 (Cell Signaling Technologies-#3033S), anti-Rabbit p65 (Cell Signaling Technologies-#4764), anti-Rabbit S177 IKK-β (Cell Signaling Technologies-#2078), anti-mouse β-actin clone AC-15 (Sigma-A5441), anti-mouse GFP B-2 clone (Santa Cruz-sc-9996), anti-Rabbit Dab2 H-110 clone (Santa Cruz-sc13982), anti-Rabbit TRAF6 clone H-274 (Santa Cruz-sc7221), IκB-alpha C-21 clone (Santa Cruz-sc371). For TransAM® EMSA, nuclear lysates were separated using the NE-PER kit (Pierce). 10 µg of nuclear lysate was used to assess DNA binding in the TransAM EMSA according to the manufacturer's protocol (Active Motif). For protein stability assays, cells were incubated in serum-reduced media (2% FBS DMEM) supplemented with 50 mg/ml cycloheximide (Sigma Aldrich-C48591ML) for a time course up to 10 h. Cells were chilled, washed with cold PBS three times and lysed directly into 2x SDS Laemmli Sample Buffer before separation by SDS-PAGE.

Immunofluorescence Confocal Microscopy- Cells were plated on coverslips and treated as indicated. Briefly, cells were rinsed in PBS and fixed in 4% paraformaldehyde, blocked with blocking buffer (1X PBS, 5% Gelatin, 0.25% Triton X-100 and 0.5% BSA) for 15 min at room temperature. Cells were stained with indicated primary antibody (3h, RT), washed thrice and then stained in secondary antibody. After washing, the cells were stained with DAPI and mounted on slides. The slides were stored in the dark (4^{o}C) until imaging. Images were taken using an Olympus FluoView FV1000 Confocal Microscope.

Quantitative real time RT-PCR- RNA was isolated from cells using the RNeasy kit (Qiagen). cDNA was reverse transcribed from RNA using Bio-Rad iScript cDNA Synthesis Kit (BioRad-1708891). PCR Primers were designed using NCBI-Primer Blast (http://www.ncbi.nlm.nih.gov/tools/primer-blast); sequences are shown in Table 1. QRT-PCR was performed using the SYBR GreenER kit (Invitrogen) or SensiMix SYBR Fluorescein kit (Bioline-QT615-02). β2-microglobulin (*β2m*) was used for normalization. PCR efficiency was determined for each primer pair using a dilution series of a typical sample of cDNA. The relative quantification of gene expression was performed as previously described(6).

Blood cell analysis- Peripheral whole blood was taken from the tails of *Dab2*$^{fl/fl}$ and *Dab2*$^{fl/fl}$*LysM*^{Cre} mice and analyzed by Hemavet (Drew Scientific). For flow cytometry, freshly isolated peripheral blood was treated with ammonium chloride for 5 min to remove RBC and then resuspended in FACS buffer containing PBS, 2% FBS, 10 mM EDTA, and 0.01% NaN_3. Cell suspensions were blocked with anti–mouse CD16/32 followed by incubation with specific mAbs [or fluorescence minus one (FMO)] controls for 20 min at 4°C. Flow cytometry was performed on FACSCanto II flow cytometer (BD), and data were analyzed using FlowJo (Tree Star, Inc.). Antibodies for surface staining: Ly6C (FITC), CD45 (APC-Cy7), CD11b (PerCP-Cy5.5), Ly6G (APC), SiglecF (PE) and CD11c (PE-Cy7) were all from BD Bioscience.

TRAF6 sequence domain screen- Human Dab2 (NP_001334.2) and mouse Dab2 (NP_075607.2) amino acid sequences were analyzed by ELM Functional Site Prediction algorithm at www.ELM.eu.org. Putative mouse

and human TRAF6 domains in Dab2 were compared to established domains for known TRAF6-interacting proteins obtained from the provided TRAF6 information link.

Collection and analysis of human bronchoalveolar lavage- Bronchoalveolar lavage samples were obtained from critical care patients at the University of Virginia Hospital in accordance with the Institutional Review Board. Samples were obtained from 4 male and 2 female patients ages 44 to 71 (Median: 58) who underwent bronchoalveolar lavage due to acute respiratory distress syndrome (ARDS) or pneumonia. Samples were kept at 4°C and spun down at 1500 rpm for 5 min. Red blood cells were lysed by incubation of cell pellet with 0.83% ammonium chloride for 10 min at room temperature. Cells were prepared for flow cytometry as above and stained with the following antibodies: Human TruStainFcX (Biolegend 422302), CD163-PE-CF591 (BD Biosciences 562670), CD14-APC-Cy7 (BD Biosciences 55781), CD206-PE (BD Pharmingen 555954), dab2 (Abcam ab76253), goat anti-rabbit IgG-Pacific Blue (Molecular Probes, P10994). Experimenter was blinded to all patient information.

Table 1-PCR primers

Gene Name	Forward Primer Sequence	Reverse Primer Sequence
Dab2	CTCAGGGACAACACAAGCAA	AAATTGATGCTGGCCTTCAC
p96 Dab2	GACATGTCTACACCTCCTGACCT	AGGATGCCTGAGGCTTTGGTCG
p67 Dab2	GACATGTCTACACCTCCTGACC	TGGGGCAGGAGCATTGCCTTT
Il6	CCACGGCCTTCCCTACTTCA	TGCAAGTGCATCATCGTTGTTC
Tnfα	GAACTGGCAGAAGAGGCACT	AGGGTCTGGGCCATAGAACT
IL1b	TACCAGTTGGGGAACTCTGC	CAAAATACCTGTGGCCTTGG
β2M	GCTATCCAGAAAACCCCTCAAATTCA	GCAGGCGTATGTATCAGTCTCAGTG
Il10	CCAAGGTGTCTACAAGGC	TAGAATGGGAACTGAGGTATC
Ccl2	CTTCTGGGCCTGCTGTTCA	AGCCTACTCATTGGGATCA
Arg1	AAGACAGCAGAGGAGGTGAAGAG	TGGGAGGAGAAGGCGTTTGC
Mgl1	CTGGATCCTGGTGTCTTGGT	AGGTGGGTCCAAGAGAGGAT
Ym1	CTTCCACACAGGAGCAGGAATC	GCTCCATGGTCCTTCCAGTA
Mrc1	CAAGGAAGGTTGGCATTTGT	CCAGGCATTGAAAGTGGAGT
Emr1	GACAATTGGGATCTGCCCTA	GGCCCTCCTCCACTAGATTC
Icsbp/Irf8	TGACACCAACCAGTTCATCCGAGA	TGCTCTACCTGCACCAGAATGAGT
Cd68	TGGGCCAAAGCTTCTGCTGT	GGAGGACCAGGCCAATGATG
Ifnγ	TTGATGATGACCCTGTGCCTTGG	GATTCTGAAGTGCTGCGTTGATGG
Il4	TGTCATCCTGCTCTTCTTTCTC	TCTGTGGTGTTCTTCGTTGC
Il12	CTCCTCTTCCCTGTCGCTAAC	CAGTCCACCTCTACAACATAAACG
Mgl2	GACTGAGTTCTCGCCTCTGG	AGGTGGGTCCAAGAGAGGAT
Nos2	TGTTAGAGACACTTCTGAGGCTC	CACTTTGGTAGGATTTGACTTT

REFERENCES

1. Kadl, A., Meher, A.K., Sharma, P.R., Lee, M.Y., Doran, A.C., Johnstone, S.R., Elliott, M.R., Gruber, F., Han, J., Chen, W., et al. 2010. Identification of a novel macrophage phenotype that develops in response to atherogenic phospholipids via Nrf2. *Circ. Res.* 107:737-746.
2. Liang, J., Song, W., Tromp, G., Kolattukudy, P.E., and Fu, M. 2008. Genome-wide survey and expression profiling of CCCH-zinc finger family reveals a functional module in macrophage activation. *PLoS One* 3:e2880.
3. Louvet, A., Teixeira-Clerc, F., Chobert, M.N., Deveaux, V., Pavoine, C., Zimmer, A., Pecker, F., Mallat, A., and Lotersztajn, S. 2011. Cannabinoid CB2 receptors protect against alcoholic liver disease by regulating Kupffer cell polarization in mice. *Hepatology* 54:1217-1226.
4. Zhou, L., Ma, Q., Shi, H., and Huo, K. 2010. NUMBL interacts with TRAF6 and promotes the degradation of TRAF6. *Biochem. Biophys. Res. Commun.* 392:409-414.
5. Ma, Q., Zhou, L., Shi, H., and Huo, K. 2008. NUMBL interacts with TAB2 and inhibits TNFalpha and IL-1beta-induced NF-kappaB activation. *Cell. Signal.* 20:1044-1051.
6. Pfaffl, M.W. 2001. A new mathematical model for relative quantification in real-time RT-PCR. *Nucleic Acids Res.* 29:e45.

Supplemental Figure 1: *Dab2* expression is differentially regulated in M1 and M2 macrophages

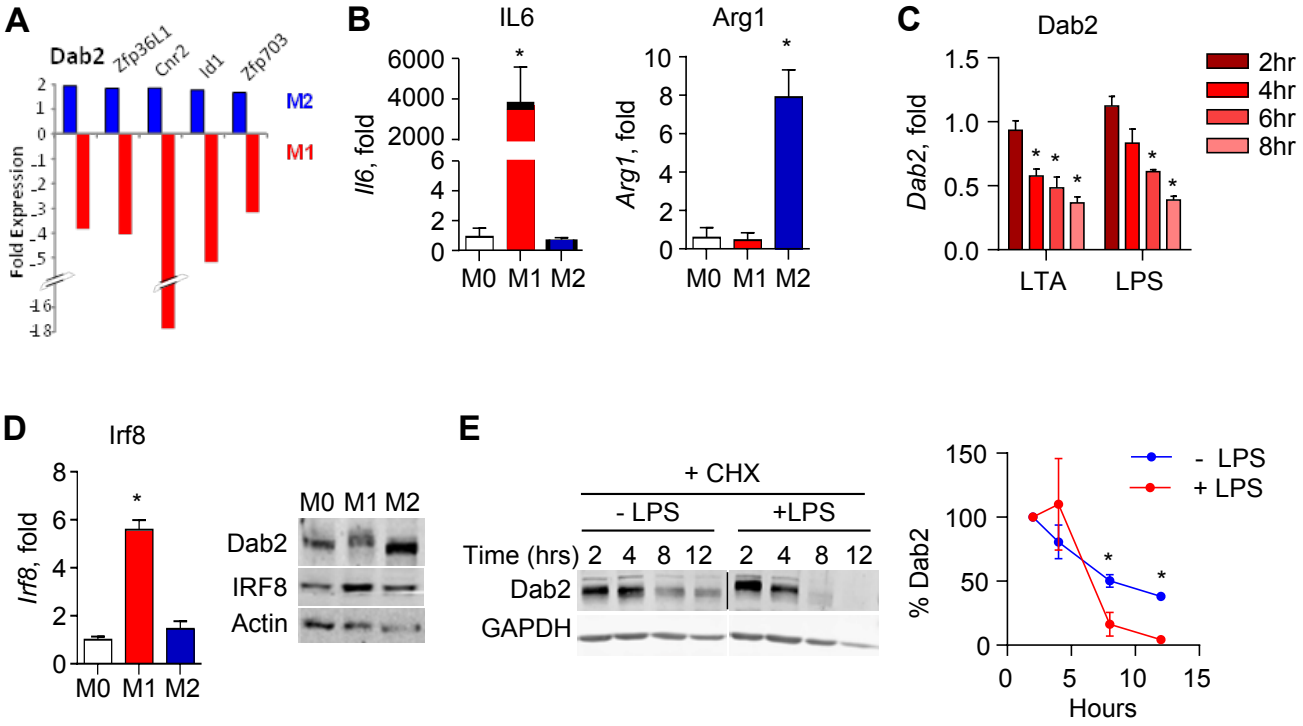

Supplemental Figure 1: *Dab2* expression is differentially regulated in M1 and M2 macrophages.

(**A**) Microarray analysis was performed after treating BMDM with either M1 stimuli LPS and IFNγ, or the M2 stimulus IL-4 for 3 hours(1). Screening for genes that are differentially regulated in M1 and M2 macrophages revealed *Dab2* among a group of genes that are upregulated in M2, but downregulated in M1 macrophages (also including the zinc finger protein Zfp36L1, cannabinoid receptor 2, inhibitor of differentiation Id1, and Zfp703, some of which have previously been implicated in the control of macrophage activation(2) (3)). (**B**) *Il6* (M1 marker) and *Arg1* (M2 marker) expression were quantified and normalized to *β2m mRNA*. Results are presented as relative to those of M0. Data are representative of 3 independent experiments. *$P < 0.05$ students t-test (mean ± s.e.m. of quadruplicate treatments). (**C**) *Dab2* expression was measured in BMDM isolated from a C56Bl/6 mouse and treated with 10 µg/ml LTA or 1 µg/ml LPS for up to 8hr. Results are normalized to *β2m* mRNA and are presented as relative to untreated cells. *P<0.0006 by 2-way ANOVA with Sidak's multiple comparison test. (**D**) *Irf8* mRNA (left) and protein (right) expression was quantified in RAW 264.7 M0, M1, and M2 polarized macrophages. Western blot (right) demonstrates dab2 protein levels in M0, M1, and M2 polarized RAW 264.7 macrophages (8 h). Actin serves as a loading control. (**E**) Dab2 protein stability was measured by immunoblot of lysates of RAW 264.7 macrophages that were untreated or treated with 100 ng/ml LPS in the presence of 10 µg/ml cycloheximide, a protein synthesis inhibitor over a 12 h time course. GAPDH serves as a loading control. Quantification of three independent experiments is shown on the right. *P<0.05 by student's t-test.

Supplemental Figure 2: *Dab2* expression in knockdown and overexpression systems

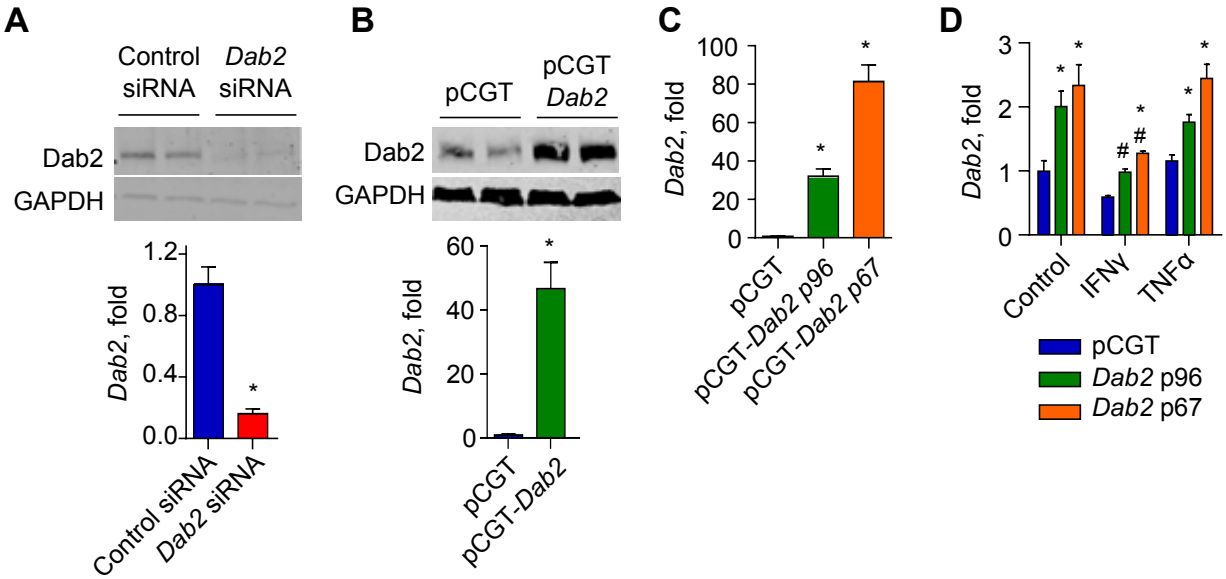

Supplemental Figure 2: Manipulation of Dab2 expression by siRNA and expression plasmids. (**A**) RAW 264.7 macrophages were transfected with control or *Dab2* siRNA for 48 h. *Upper pane l*- Immunoblot analysis of Dab2 protein expression with GAPDH serving as a loading control. *Lower panel* - qRT-PCR analysis of *Dab2* mRNA expression, normalized to *β2m* mRNA. Data is presented as mean ± s.e.m. of quadruplicate treatments. (**B**) RAW264.7 macrophages were transfected with pCGT or pCGT-Dab2 for 48 h. *Upper panel* - Immunoblot analysis of Dab2 protein expression with GAPDH serving as a loading control. *Lower panel* - qPCR analysis of *Dab2* mRNA expression was normalized to *β2m* mRNA. Data is presented as mean ± s.e.m. of quadruplicate treatments. (**C**) qPCR analysis of *Dab2* levels normalized to *β2m* in resting cells transfected with pCGT, *p67 Dab2,* or *p96 Dab2*. (**D**) qPCR analysis of *Dab2* levels normalized to *β2m* in RAW 264.7 macrophages transfected with pCGT, *p67 Dab2,* or *p96 Dab2* and treated with IFNγ for 16 h or TNFα for 4 h. *P<0.05 significantly different from pCGT. #P<0.05 significantly different from control.

Supplemental Figure 3: Analysis of cellular composition of blood in Dab2$^{fl/fl}$ and Dab2$^{fl/fl}$ LysM^{Cre} mice

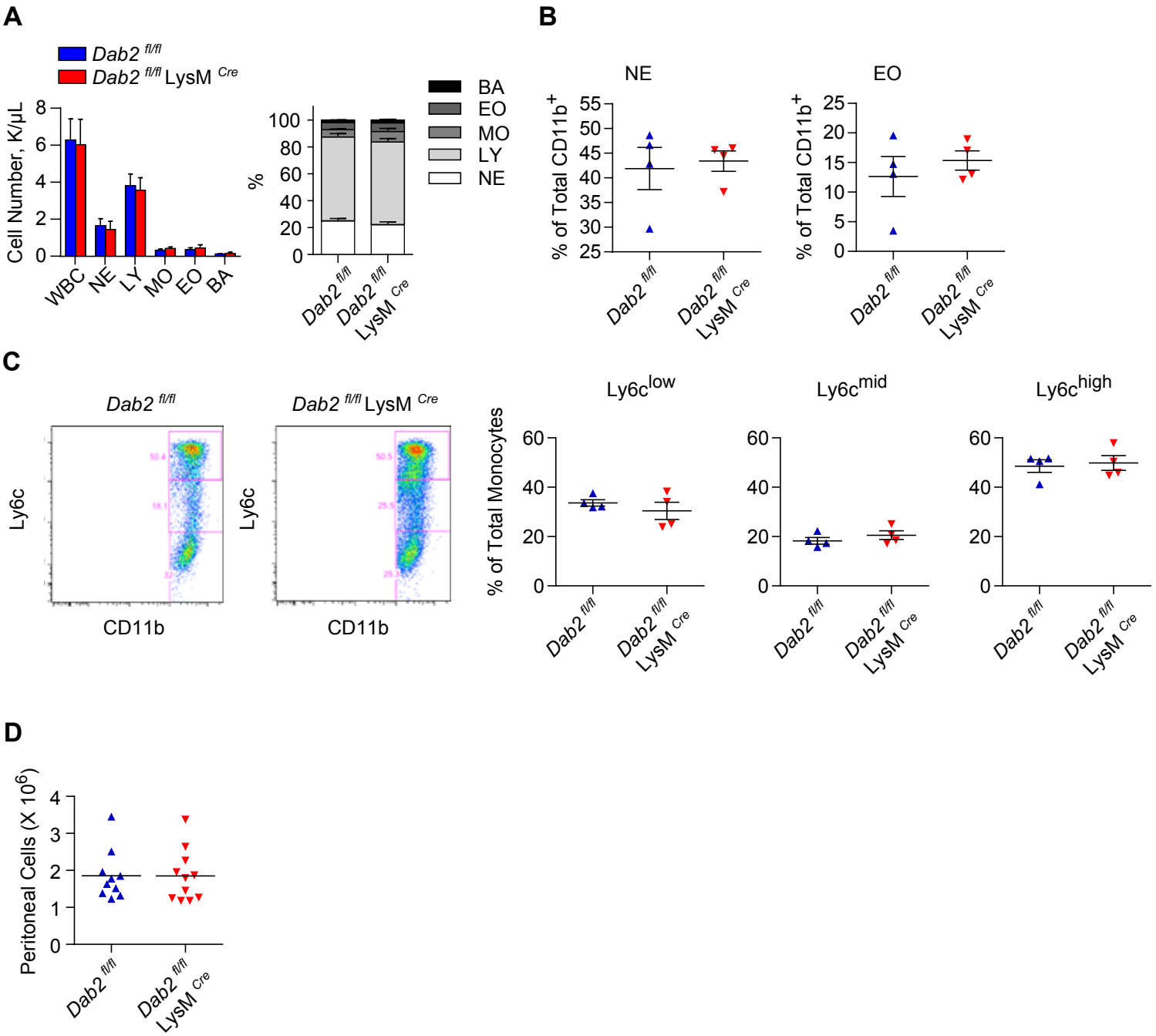

Supplemental Figure 3: Analysis of cellular composition of blood in *Dab2$^{fl/fl}$* and *Dab2$^{fl/fl}$LysM^{Cre}* mice. Whole blood composition was examined by Hemavet analyzer. (**A**) Cell number in K/µl and percent distribution of white blood cells (WBC), neutrophils (NE), lymphocytes (LY), monocytes (MO), eosinophils (EO), and basophils (BA). Data are shown as mean ± s.e.m.; n = 7 *for Dab2$^{fl/fl}$*, n = 6 for *Dab2$^{fl/fl}$LysM^{Cre}*. (**B and C**) White blood cells stained with CD45-APC-Cy7, CD11b-PerCP-Cy5.5, Ly6G-APC, Siglec F-PE, and Ly6C-FITC were subjected to FACS analysis. (**B**) Percentage of CD45$^+$CD11b$^+$Ly6G$^+$ (neutrophils NE; n=4), and CD45$^+$CD11b$^+$SiglecF$^+$ (eosinophils EO; *n* = 4) cells. Data is presented as mean ± s.e.m. (**C**) Representative gating of CD45$^+$CD11b$^+$Ly6c-SSC^{lo} monocytes analyzed for Ly6c^{hi}, Ly6c^{int}, Ly6c^{lo} expression (left two panels). Data points shown in the quantification (right three panels) represent individual animals (mean ± s.d. *n* = 4). (**D**) Peritoneal lavage cell number as determined by hemocytometer from LPS treated *Dab2$^{fl/fl}$* and *Dab2$^{fl/fl}$LysM^{Cre}* mice. Each point represents one mouse. Data is expressed as mean +/- s.e.m.

Supplemental Figure 4: TNFα and Palmitate treatment of Dab2 null macrophages results in increased inflammatory gene expression

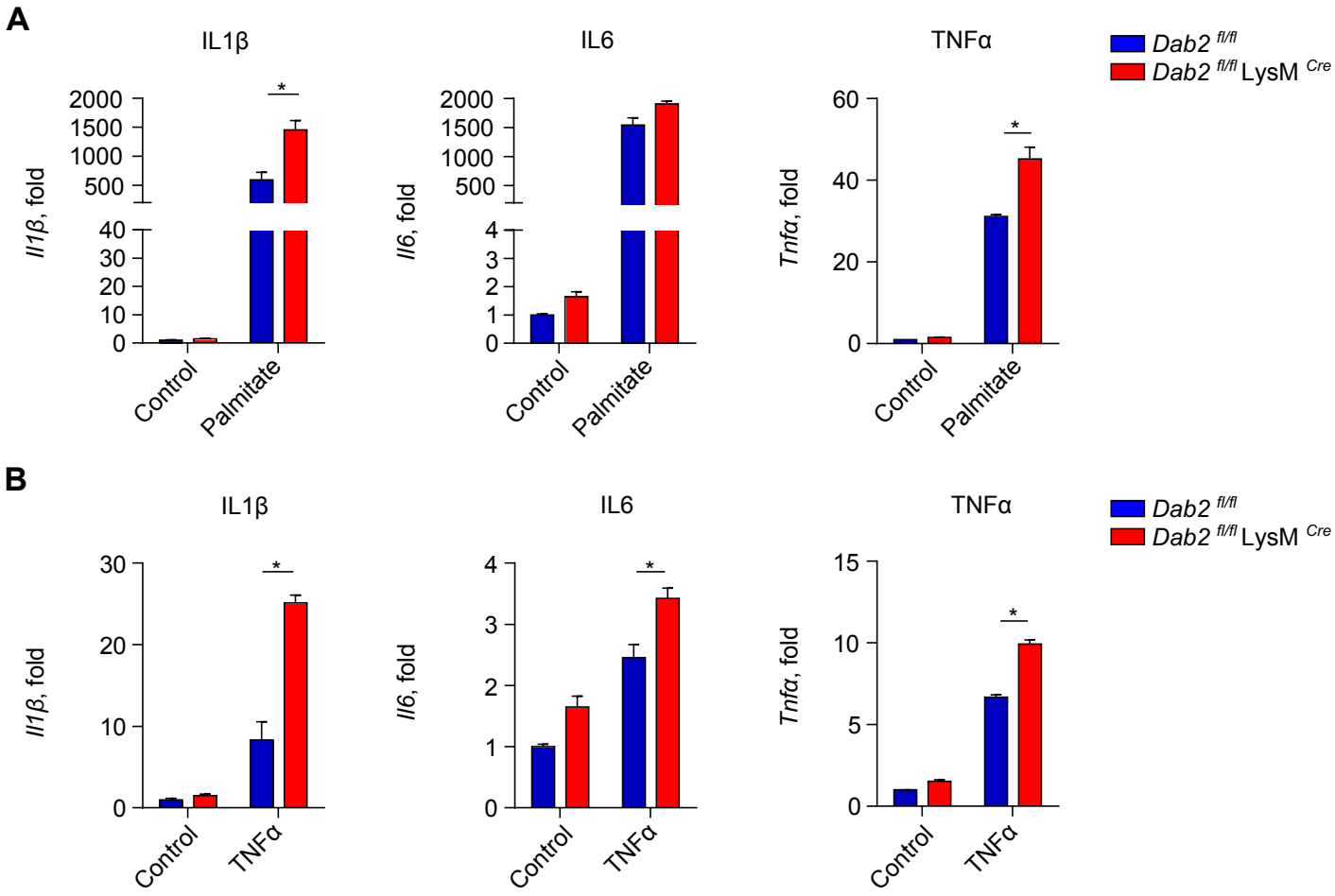

Supplemental Figure 4: Quantitative RT-PCR analysis of *Il1β*, *Il6*, and *Tnfα* mRNA expression in *Dab2*$^{fl/fl}$ and *Dab2*$^{fl/fl}$*LysM*^{Cre} BMDM treated for 6 h with 200 μM palmitate (**A**) or 100 ng/ml TNFα (**B**). Results are normalized to *β2m*. *P<0.05 by student's t-test.

Supplemental Figure 5:

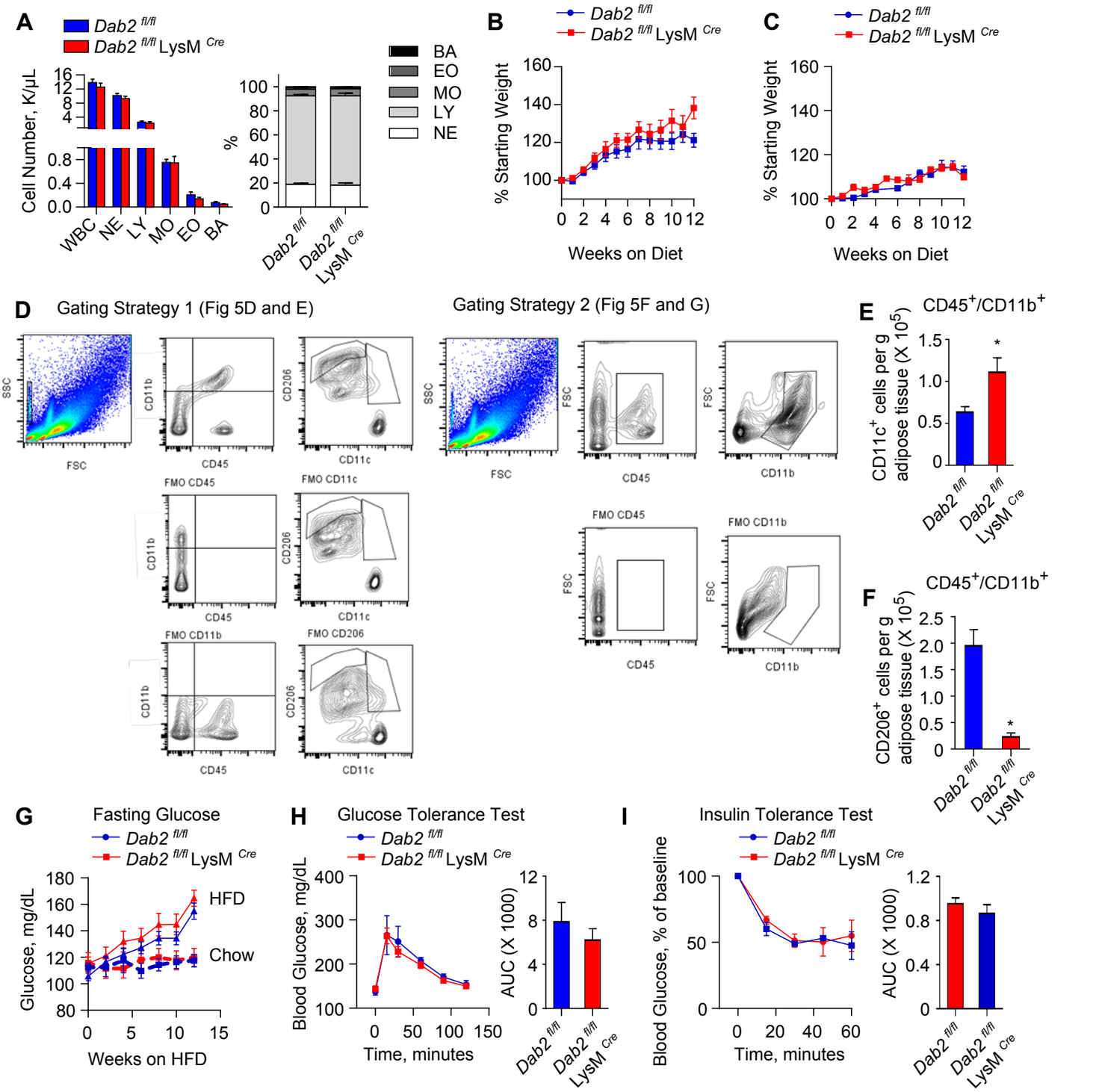

Supplemental Figure 5: (**A**) *Dab2*$^{fl/fl}$ and *Dab2*$^{fl/fl}$*LysM*^{Cre} mice (n = 8 and n = 6, respectively) were fed a high fat diet [60% kcal from fat, 0.2% cholesterol (Bioserv)] for 12 weeks and blood was analyzed for WBC content by Hemavet, revealing no difference in absolute cell numbers or distribution. (**B** and **C**) Weight gain is shown for high fat diet fed, female *Dab2*$^{fl/fl}$ (n=14) and *Dab2*$^{fl/fl}$*LysM*^{Cre} (n=9) mice (**B**) and age-matched, chow fed, female *Dab2*$^{fl/fl}$ (n=5) and *Dab2*$^{fl/fl}$*LysM*^{Cre} (n=6) mice (**C**). (**D**) Flow cytometry gating strategy for isolated cells from adipose stromal vascular fraction: Cells were stained with CD45-APC-Cy7, CD11b-FITC, CD206-PE and CD11c-AF647 antibodies. Gating strategy 1 (for Fig 5D and E) shows cells gated by CD45$^+$/CD11b$^+$ (corresponding FMOs shown below). Next, CD45$^+$/CD11b$^+$ cells were assessed by CD11c$^+$ versus CD206$^+$ and gated as CD11c$^+$ or CD206$^+$ based on corresponding FMOs shown below. MFI for either CD11c or CD206 was determined for CD45$^+$/CD11b$^+$ cells. Gating Strategy 2 (for Fig 5F and G): First, CD45$^+$ cells were gated (CD45 FMO shown below) and next gated by CD11b$^+$ (CD11b FMO shown below). (**E**) Absolute number of CD45$^+$/CD11b$^+$/CD11c$^+$ cells per gram adipose tissue processed. (**F**) Absolute number of CD45$^+$/CD11b$^+$/CD206$^+$ cells per gram adipose tissue processed. For (**E**,**F**) data is presented as mean ± s.e.m. *P < 0.05 by Student's t-test. (**G**) *Dab2*$^{fl/fl}$ and *Dab2*$^{fl/fl}$*LysM*^{Cre} mice were fed either a regular chow (Teklad) (n = 5 and n = 6, respectively) or a high fat diet [60% kcal from fat, 0.2% cholesterol (Bioserv)] (n = 9 and n = 14, respectively) for 12 weeks. Fasting glucose levels were measured every other week over the time of feeding by glucometer sampling of tail blood after 6 hour fast. (**H**) Glucose tolerance tests and (**I**) insulin tolerance tests in *Dab2*$^{fl/fl}$ and *Dab2*$^{fl/fl}$*LysM*^{Cre} mice that were fed a regular chow diet. Mice were fasted 6 hours and injected intraperitoneally (i.p.) with a 1 g/kg glucose bolus for glucose tolerance test or 0.75 U/kg insulin for insulin tolerance test at time 0, and blood glucose levels were measured from tail blood by glucometer. Data was analyzed by area under the curve (AUC) analysis revealing no difference in glucose tolerance between chow fed *Dab2*$^{fl/fl}$ mice and *Dab2*$^{fl/fl}$*LysM*^{Cre} mice. Data is presented as mean ± s.e.m. (n = 5 or 6 for GTT, n = 3 for ITT).

Supplemental Figure 6: Dab2 does not enter the nucleus of macrophages upon LPS treatment

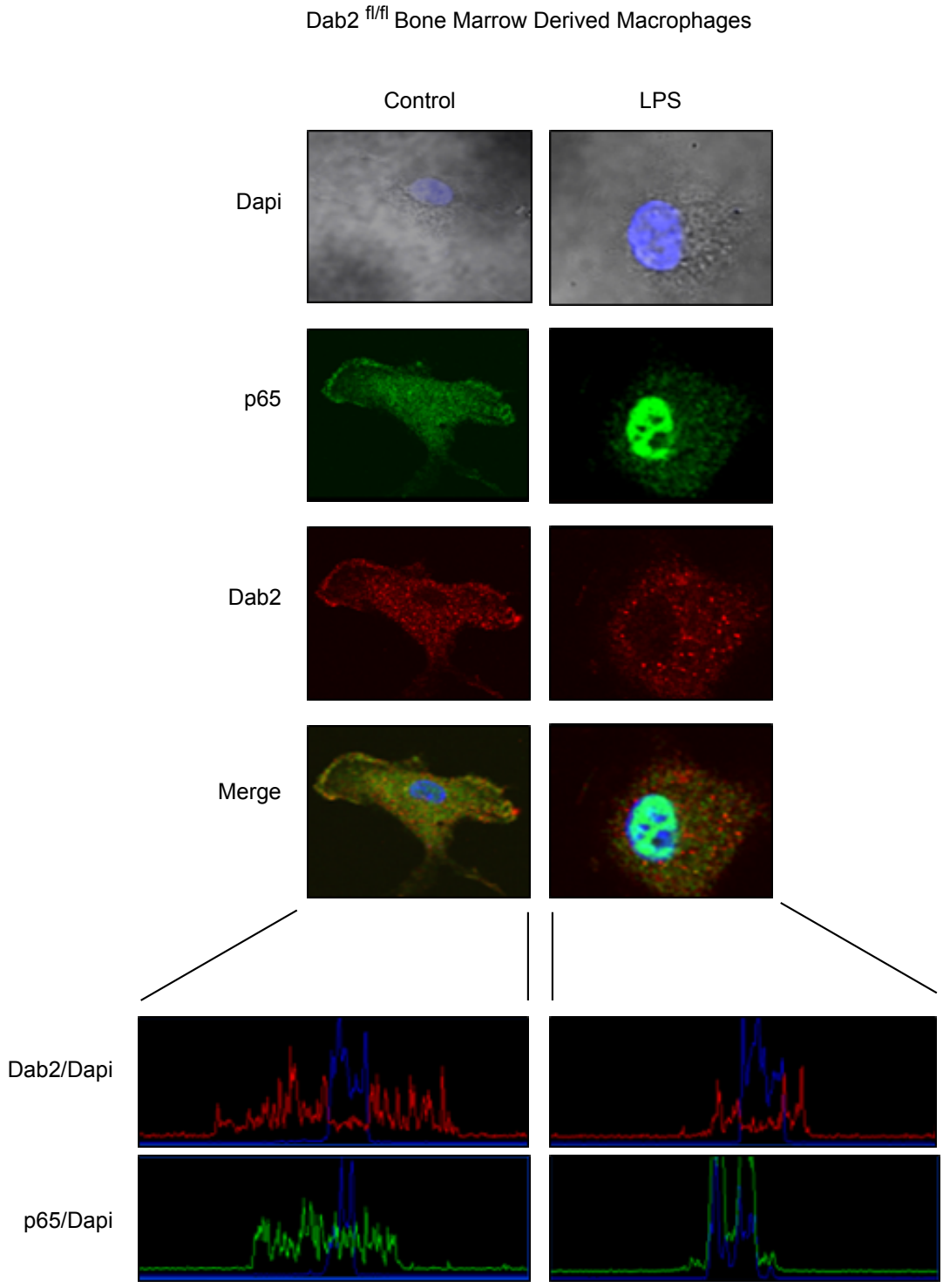

Supplemental Figure 6: Confocal microscopy of control and LPS treated bone marrow-derived macrophages isolated from *Dab2*$^{fl/fl}$ mice shows nuclei in blue (Dapi), p65 in green, and Dab2 in red. Bottom panels represent analysis of z-stack images such that the y-axis is intensity of staining. Blue lines represent Dapi staining and show a peak in the middle, representing the nucleus. In untreated macrophages, p65 staining (green line) is evenly distributed along the cell, while in LPS treated macrophages, p65 staining (green line) aligns with Dapi staining (blue line), indicating the presence of p65 in the nucleus in LPS-treated macrophages. Dab2 staining (red line) is evenly distributed along the cell in both untreated and LPS-treated macrophages, indicating that Dab2 does not enter the nucleus upon LPS treatment.

Supplemental Table 1

TRAF6 binding site consensus sequence: **P** X **E** X X **[F Y W H D E]**

	Site 1		Site 2	
DAB2 *Mus musculus*	226-234	NS**P**T**E**SK**D**I	689-697	GI**P**Q**E**HV**D**H
DAB2 *Homo sapiens*	226-234	NS**P**T**E**SK**D**I	691-699	GI**P**Q**E**NA**D**H
NUMBL *Mus musculus*	269-277	TS**P**G**E**KG**E**A	569-577	LD**P**F**E**AQ**W**A
NUMBL *Homo sapiens*	269-277	TS**P**G**E**KG**E**A	574-582	LD**P**F**E**AQ**W**A

Supplemental Table 1: TRAF6 binding site consensus sequence in shown as well as two putative TRAF6 binding sites in murine Dab2 at amino acid position 226 and 689 which are conserved in human Dab2. NUMBL is a related TRAF6-binding adaptor protein that contains two conserved TRAF6 binding sites(4, 5).